Proceedings of the ASME 2016 International Mechanical Engineering Congress and Exposition
IMECE2016
November 11-17, 2016, Phoenix, Arizona, USA

IMECE2016-65645

COMPONENT-WISE MODELS FOR THE ACCURATE DYNAMIC AND BUCKLING ANALYSIS OF COMPOSITE WING STRUCTURES

E. Carrera, A. Pagani*
Department of Mechanical and Aerospace Engineering
Politecnico di Torino
Corso Duca degli Abruzzi 24, 10129 Torino, Italy

P. H. Cabral, A. Prado, G. Silva
Embraer S.A.
12227-901 São José dos Campos
Brazil

ABSTRACT

In the present work, a higher-order beam model able to characterize correctly the three-dimensional strain and stress fields with minimum computational efforts is proposed. One-dimensional models are formulated by employing the Carrera Unified Formulation (CUF), according to which the generic 3D displacement field is expressed as the expansion of the primary mechanical variables. In such a way, by employing a recursive index notation, the governing equations and the related finite element arrays of arbitrarily refined beam models can be written in a very compact and unified manner. A Component-Wise (CW) approach is developed in this work by using Lagrange polynomials as expanding cross-sectional functions. By using the principle of virtual work and CUF, free vibration and linearized buckling analyses of composite aerospace structures are investigated. The capabilities of the proposed methodology and the advantages over the classical methods and state-of-the-art tools are widely demonstrated by numerical results.

NOMENCLATURE

F_τ Cross-sectional expanding functions.
$\mathbf{K}^{ij\tau s}$ Fundamental nucleus of the linear stiffness matrix.
$\mathbf{K}^{ij\tau s}_{\sigma^0}$ Fundamental nucleus of the geometrical stiffness matrix.
$\mathbf{I}$ Identity matrix.
L Beam length.
L_{int} Internal strain energy.
L_{σ^0} Work of the initial stresses.
M Number of expansion terms.
N_i Shape functions.
V Beam volume, $V = \Omega \times L$.
p polynomial order of the shape functions.
$\mathbf{q}_{\tau i}$ FE nodal unknowns.
$\mathbf{u}$ Displacement vector.
$\mathbf{u}_\tau$ Generalized displacement vector.
δ Virtual variation.
$\boldsymbol{\varepsilon}$ Strain vector.
Ω Beam cross-section domain.
$\boldsymbol{\sigma}$ Stress vector.
$\boldsymbol{\sigma}^0$ Initial stress state vector.
$(\,)_i$ Finite element expansion index on the variable.
$(\,)_j$ Finite element expansion index on the variation.
$(\,)_s$ Cross-sectional expansion index on the variation.
$(\,)_\tau$ Cross-sectional expansion index on the variable.

INTRODUCTION

The availability of appropriate tools for the accurate dynamic and buckling analysis of metallic and composite aerospace structures is of fundamental importance for the design and sizing processes. These structures, which are essentially reinforced-shells (see [1, 2]), are commonly modelled by combining, via rigid links (e.g. through Lagrange multipliers), one-dimensional (1D/beam) and two-dimensional (2D/shell) finite elements that are implemented in commercial codes. This approach, however, introduces various physical and geometrical inconsistencies, see [3–5]. For example, the out-of-plane warping of the

*Corresponding author, email: alfonso.pagani@polito.it

stringers and the transverse normal stress in the panels, eventually, are not considered. Nowadays, the only way to overcome these issues is to utilize either ad-hoc methodologies or 3D/solid finite element models, which can seriously affect the efficiency of the analysis.

In the present work, a geometrically consistent higher-order beam model able to characterize in a correct way the three-dimensional strain and stress fields is proposed for the accurate free vibration and buckling analyses of reinforced and composite aerospace structures. One-dimensional models are formulated by utilizing the well-known Carrera Unified Formulation (CUF), according to which the generic 3D displacement field is the expansion, through generic cross-sectional functions, of the generalized displacement unknowns [6, 7]. CUF, by employing a recursive index notation, allows the governing equations and, eventually, the corresponding finite element matrices of higher-order beam models to be written in a very compact and unified manner. According to Carrera *et al.* [8–12] and Carrera and Pagani [13], a Component-Wise (CW) approach is formulated in this paper by using Lagrange polynomials as expanding cross-sectional functions. Along the axis of the beam, on the other hand, the problem domain is approximated by a classical finite element procedure. The CW approach allows the analyst to model, readily, each structural component (stringers, panels, ribs, spars, etc.) by using the same formulation (i.e., the same 1D finite element) and tune the theory accuracy by opportunely refining the kinematic characteristics at the cross-sectional level. By using the principle of virtual work and CUF, free vibration and linearized buckling analyses of composite and reinforced aerospace structures are investigated by CW models. Particular attention is given to the buckling formulation, which makes use of the complete 3D stress field and Green-Lagrange strains for the development of the linearized tangent/geometrical stiffness contribution.

This paper is organized as follows: (i) first, CUF is briefly introduced; (ii) then, CUF is utilized along with a finite element procedure to develop the fundamental nuclei of the linear and geometrical stiffness matrix which are employed in the linearized buckling analyses; (iii) next, numerical results are discussed in details and both reinforced panels and composite wing box structures are considered; (iv) finally, the main conclusions are drawn.

CARRERA UNIFIED FORMULATION

We consider a beam structure whose cross-section (Ω) lies on the xz-plane of a generic Cartesian reference system. The boundaries of the problem along the axis y are $0 \leq y \leq L$, where L is the length of the beam. Within the framework of the Carrera Unified Formulation (CUF), the displacement field $\mathbf{u}(x,y,z)$ can be expressed as a generic expansion of the primary unknowns:

$$\mathbf{u}(x,y,z) = F_\tau(x,z)\mathbf{u}_\tau(y), \qquad \tau = 1,2,....,M \tag{1}$$

where F_τ are the functions of the coordinates x and z on the cross-section, $\mathbf{u}_\tau$ is the vector of the *generalized displacements*, M stands for the number of the terms used in the expansion, and the repeated subscript, τ, indicates summation. The choice of F_τ determines the class of the 1D CUF model that is required and subsequently to be adopted.

Taylor Expansion (TE) 1D CUF models consists of McLaurin series that uses the 2D polynomials $x^i\, z^j$ as F_τ basis, see [6]. For instance, the second-order TE beam model presents the following kinematics:

$$\begin{aligned} u_x &= u_{x_1} + x\, u_{x_2} + z\, u_{x_3} + x^2\, u_{x_4} + xz\, u_{x_5} + z^2\, u_{x_6} \\ u_y &= u_{y_1} + x\, u_{y_2} + z\, u_{y_3} + x^2\, u_{y_4} + xz\, u_{y_5} + z^2\, u_{y_6} \\ u_z &= u_{z_1} + x\, u_{z_2} + z\, u_{z_3} + x^2\, u_{z_4} + xz\, u_{z_5} + z^2\, u_{z_6} \end{aligned} \tag{2}$$

where the parameters on the right-hand side (u_{x_1}, u_{y_1}, u_{z_1}, u_{x_2}, etc.) are the unknown generalized displacements of the beam axis as functions of the y-axis. It should be noted that classical beam models (e.g., Euler-Bernoulli and Timoshenko beam models) are degenerated cases of the linear TE model.

In this paper, Lagrange polynomials are used as F_τ cross-sectional functions. The resulting beam theories are called LE (Lagrange Expansion) CUF models in the literature [7]. Lagrange polynomials as used in this paper can be found in [14]. In the framework of CUF, linear three- (L3) and four-point (L4), quadratic six- (L6) and nine-point (L9), as well as cubic 16-point (L16) Lagrange polynomials have been used to formulate linear to higher-order kinematics beam models. For example, the kinematics of the quadratic beam theory derived from the adoption of one single L9 polynomial set to approximate the cross-sectional displacements is:

$$\begin{aligned} u_x &= L_1\, u_{x_1} + L_2\, u_{x_2} + ... + L_9\, u_{x_9} \\ u_y &= L_1\, u_{y_1} + L_2\, u_{y_2} + ... + L_9\, u_{y_9} \\ u_z &= L_1\, u_{z_1} + L_2\, u_{z_2} + ... + L_9\, u_{z_9} \end{aligned} \tag{3}$$

where L_1, L_2, ..., L_9 are the nine Lagrange polynomials as functions of the cross-sectional coordinates. u_{x_1}, u_{y_1}, u_{z_1}, ..., u_{z_9} are functions of the coordinate y and represent the pure displacement components at the nine roots of the L9 polynomial set. For improving further the beam kinematics and obtaining a geometrically exact (isoparametric) description of complex cross-section beams, a combination of Lagrange polynomials can be used in a straightforward manner by employing CUF. For more details about LE beam theories, interested readers are referred to Carrera and Petrolo [15].

LE models have been recently used for the Component-Wise (CW) analysis of aerospace [8,9] and civil engineering constructions [13] as well as for composite laminates [10] and box structures [11, 12]. In fact, since LE utilizes only the physical boundaries to define the problem geometry, they allow the formulation

of geometrically consistent (isogeometric) models. The main advantage of the CW models is that each component of the structure can be modeled with the same finite element, whose kinematics can be opportunely enriched depending on the problem characteristics and analysis needs. Moreover, since the same higher-order formulation is used for each component, there is no need to couple components with different geometry and scales by fictitious mathematical artifices such as rigid links and MPC's (see [8]).

FINITE ELEMENT APPROXIMATION

The finite element approach is adopted here to discretize the structure along the y-axis. Thus, the generalized displacement vector $\mathbf{u}_\tau(y)$ is approximated as follows:

$$\mathbf{u}_\tau(y) = N_i(y)\mathbf{q}_{\tau i} \qquad i = 1,2,\ldots,p+1 \tag{4}$$

where N_i stands for the i-th shape function, p is the order of the shape functions, and i indicates summation. $\mathbf{q}_{\tau i}$ is vector of the FE nodal parameters.

Fundamental nucleus of the linear stiffness matrix.

The linear stiffness matrix $\mathbf{K}$ can be calculated from the virtual variation of the strain energy δL_{int}, which reads:

$$\delta L_{int} = < \delta \boldsymbol{\varepsilon}^T \boldsymbol{\sigma} > \tag{5}$$

where δ denotes the virtual variation; $\boldsymbol{\varepsilon}$ and $\boldsymbol{\sigma}$ are the strain and stress vectors, respectively; V is the initial volume of the structure ($V = \Omega \times L$); and $< (\cdot) >= \int_V (\cdot)\, dV$. By using the linear geometrical relations, the Hook's law, the CUF (Eqn. (1)) and Eqn. (4), the virtual variation of the internal work is written as follows:

$$\delta L_{int} = \delta \mathbf{q}_{\tau i}^T \mathbf{K}^{ij\tau s} \mathbf{q}_{sj} \tag{6}$$

$\mathbf{K}^{ij\tau s}$ is the CUF *fundamental nucleus* (FN) of the element stiffness matrix $\mathbf{K}$. The FN is a 3×3 matrix that, given the cross-sectional functions ($F_\tau = F_s$, for $\tau = s$) and the shape functions ($N_i = N_j$, for $i = j$), can be expanded by using the indexes $\tau, s = 1,...,M$ and $i, j = 1,...,p+1$ in order to obtain the elemental stiffness matrix of any arbitrarily refined beam model. In other words, by opportunely choosing the beam kinematics (i.e., by choosing F_τ as well as the number of expansion terms M) classical to higher-order beam theories and related stiffness array can be implemented in an automatic manner by exploiting the index notation of CUF. The nine components of $\mathbf{K}^{ij\tau s}$ are not reported here for the sake of brevity. They can be found in [16].

Fundamental nucleus of the geometrical stiffness matrix.

In this paper, particular emphasis is given to free vibration and linearized buckling problems. As far as linearized buckling is concerned, the *tangent stiffness matrix* can be obtained from the linearization of the virtual variation of the nonlinear internal strain energy $\delta(\delta L_{int})$, see [17, 18]. To a first-order approximation, $\delta(\delta L_{int})$ can be expressed as the sum of the contributions given by the linear stiffness as in the previous section and the virtual variation of the work of the initial stresses (or pre-stresses), $\boldsymbol{\sigma}^0$.

$$\delta(\delta L_{int}) \approx \delta \mathbf{q}_{\tau i}^T \mathbf{K}^{ij\tau s} \delta \mathbf{q}_{sj} + < \delta(\delta \boldsymbol{\varepsilon})^T \boldsymbol{\sigma}^0 > \tag{7}$$

By using CUF and FEM as in Eqns. (1) and (4) respectively, and the Green-Lagrange nonlinear strain-displacement relations [19], Eqn. (7) becomes:

$$\begin{aligned} \delta(\delta L_{int}) &\approx \delta \mathbf{q}_{\tau i}^T \mathbf{K}^{ij\tau s} \delta \mathbf{q}_{sj} + \delta \mathbf{q}_{\tau i}^T \mathbf{K}_{\sigma^0}^{ij\tau s} \delta \mathbf{q}_{sj} \\ &= \delta \mathbf{q}_{\tau i}^T \left(\mathbf{K}^{ij\tau s} + \mathbf{K}_{\sigma^0}^{ij\tau s} \right) \delta \mathbf{q}_{sj} \end{aligned} \tag{8}$$

where $\mathbf{K}^{ij\tau s}$ is the FN of the linear stiffness matrix as in Eqn. (6) and $\mathbf{K}_{\sigma^0}^{ij\tau s}$ is the FN of the geometrical stiffness matrix. $\mathbf{K}_{\sigma^0}^{ij\tau s}$ is a diagonal matrix and it is given in the following for reasons of completeness:

$$\begin{aligned} \mathbf{K}_{\sigma^0}^{ij\tau s} = \big(& < \sigma_{xx}^0 F_{\tau,x} F_{s,x} N_i N_j > + < \sigma_{yy}^0 F_\tau F_s N_{i,y} N_{j,y} > \\ & + < \sigma_{zz}^0 F_{\tau,z} F_{s,z} N_i N_j > + < \sigma_{xy}^0 F_{\tau,x} F_s N_i N_{j,y} > \\ & + < \sigma_{xy}^0 F_\tau F_{s,x} N_{i,y} N_j > + < \sigma_{xz}^0 F_{\tau,x} F_{s,z} N_i N_j > \\ & + < \sigma_{xz}^0 F_{\tau,z} F_{s,x} N_i N_j > + < \sigma_{yz}^0 F_{\tau,z} F_s N_i N_{j,y} > \\ & + < \sigma_{yz}^0 F_\tau F_{s,z} N_{i,y} N_j > \big)\, \mathbf{I} \end{aligned} \tag{9}$$

where $\mathbf{I}$ is the 3×3 identity matrix. As for the elemental linear stiffness matrix and given the cross-sectional functions F_τ and the 1D shape functions N_i, the fundamental nucleus of the geometric stiffness matrix can be expanded in an automatic way by employing CUF to give the elemental matrix for any desired beam theory. Finally, once the global matrices are assembled in the classical way of FEM, the critical buckling loads are determined as those initial stress states $\boldsymbol{\sigma}^0$ which render the tangent stiffness matrix singular; i.e., $|\mathbf{K} + \mathbf{K}_{\sigma^0}| = 0$.

For the sake of brevity, the formulation of the free vibration problem in the domain of CUF is not discussed in this work. Interested readers are referred to the book of Carrera *et al.* [7].

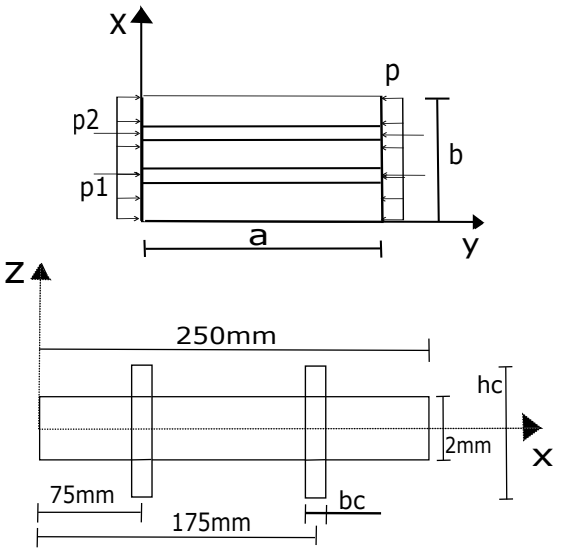

FIGURE 1. ORTHOTROPIC REINFORCED PLATE.

NUMERICAL RESULTS

In this section, selected numerical results are discussed. The main aim is to demonstrate the capability of the CW formulation to deal with simple to relatively complex geometries and anisotropy. The first example deals with the buckling analysis of an orthotropic reinforced plate. Further analyses focus on the free vibration and buckling of composite box structures, including reinforcements.

Orthotropic reinforced plate

In the first analysis case, the buckling analysis of a simply-supported orthotropic reinforced plate is discussed. The plate structure is reinforced by employing two stringers as shown in Fig. 1, where the main dimensions as well as the boundary conditions and loadings are also depicted. It should be noted that, in Fig. 1, p is a load per unit of area and $p_1 = p_2 = p \times A_c$, where A_c is the area of the stringer. The in-plane dimensions of the plate are $a = 500$ mm and $b = 250$ mm. The thickness is equal to $t = 2$ mm. The structure is entirely made of an orthotropic material with the following representative characteristics:

Elastic modula, $E_1 = 132500$ MPa; $E_2 = E_3 = 10800$ MPa.
Poisson ratios, $\nu_{12} = \nu_{13} = 0.24$, $\nu_{23} = 0.49$.
Density $\rho = 100$ kg/m^3.

Table 1 reports the first buckling loads of the structure for various dimensions of the stringers. The results by the present 1D CW model are compared to those from analytical, plane-stress solutions from Lekhnitskii [20]. The CW model employs 1D LE refined elements for each of the components of the structure (i.e., the panel and the stringers). In total, nine L9 polynomials are used to formulate the beam kinematics in accordance with CUF, whereas 20 B4 beam finite elements are utilized along the beam axis.

TABLE 1. CRITICAL BUCKLING LOADS $[\frac{N}{mm^2}]$ OF THE ORTHOTROPIC REINFORCED PLATE FOR VARIOUS DIMENSIONS OF THE STRINGERS.

$[b_c;h_c]$	[3;5]		[3;8]		[3;10]	
	Ref. [20]	CW	Ref. [20]	CW	Ref. [20]	CW
p_{cr_1}	10.4	11.9	15.2	15.6	21.1	20.1
p_{cr_2}	22.2	22.0	43.5	37.3	68.8	55.01
p_{cr_3}	46.5	43.7	84.3	75.1	150.3	130.6

It should be noted that the CW solutions agree with the reference results as the dimensions of the stringers are small. Interestingly, the difference between the 1D CW model and the plate reference model increases as the dimensions of the stringers grow. The reason is that, unlike the reference model and most of the techniques used in the literature and in practical applications for the analysis of reinforced structures, the CW model can describe the mechanics of each component of the structure separately and in an accurate manner. In fact, local phenomena and distortion involving large stringers cannot be neglected if the stringers are sufficiently large. To further underline this aspect, Fig. 2 shows the variation of the first natural frequencies as functions of the total load applied at the edge of the panel. In Fig. 2, the natural frequencies are given in the following non-dimensional form:

$$\omega^* = \omega \frac{b^2}{t} \sqrt{\frac{\rho}{E_1}} \tag{10}$$

For small stringers (Fig. 2a), the first buckling load can be recognized as the load that nullifies the natural frequency related to the mode shape shown in Fig. 3a. On the contrary, a crossing phenomena occurs in Fig. 2b where sufficiently big stringers are considered, and the first buckling mode becomes the one shown in Fig. 3b, in which the stringers deformation are visible. Of course, this behaviour cannot be detected with classical models.

Circumferentially-uniform-stiffness box beam

In the second analysis case, the free vibration characteristics of the same composite box beam as analyzed in [21] is considered. The cantilever beam is prismatic with length $L = 762$ mm, width $b = 24.21$ mm and height $h = 13.46$ mm. Each wall of the box has a total thickness equal to $t = 0.762$ mm and it is made of six equal layers. In this example, a CUS (Circumferentially Uniform Stiffness) stacking sequence $[\theta]_6$ is addressed. Each layer of the structure is made of an orthotopic material, whose density and mechanical properties along the fibre (L) and transverse (T) directions are: $\rho = 1601$ Kg/m^3, $E_L = 142$ GPa, $E_T = 9.8$

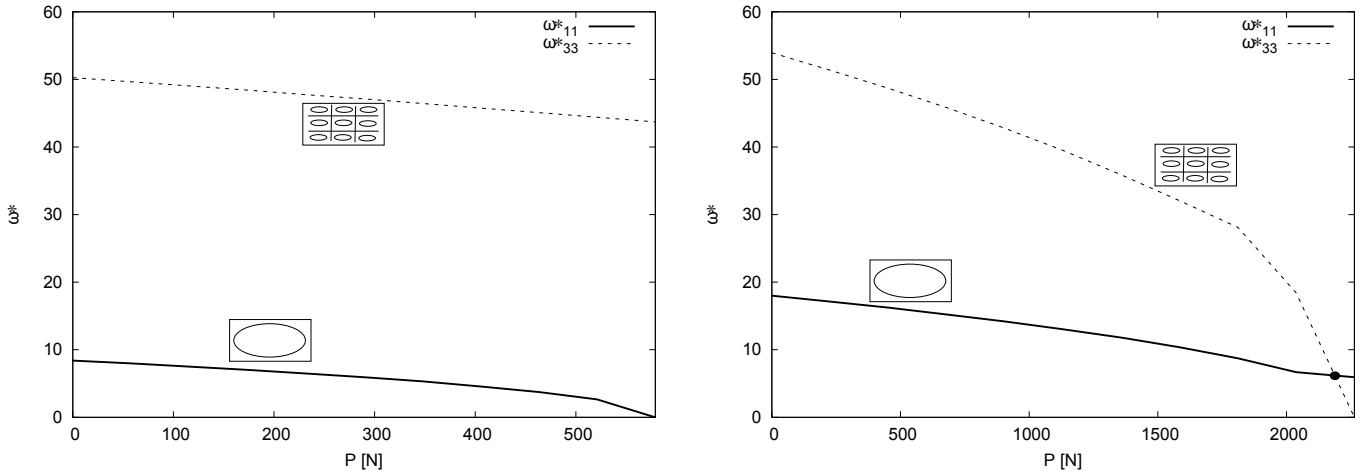

(a) h_c=12 mm (b) h_c=24 mm

FIGURE 2. VARIATION OF THE NATURAL FREQUENCIES VS PRE-STRESS, P [N]; CW MODEL.

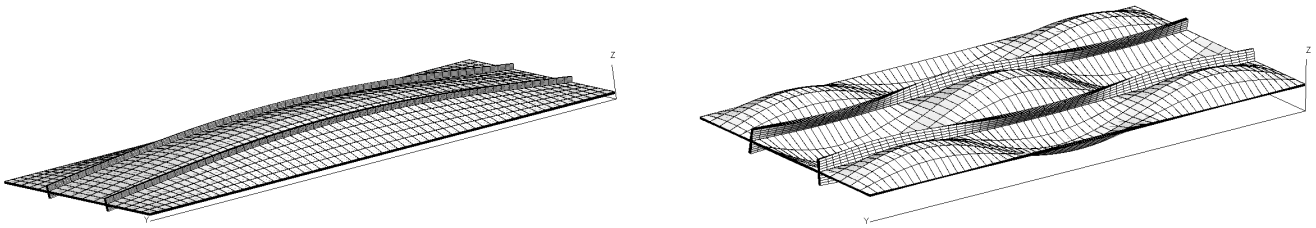

(a) h_c=12 mm (b) h_c=24 mm

FIGURE 3. FIRST BUCKLING MODE OF THE ORTHOTROPIC REINFORCED PANEL FOR DIFFERENT DIMENSIONS OF THE STRINGERS; CW MODEL.

GPa, $G_{LT} = 6.0$ GPa, $G_{TT} = 4.83$ GPa, $\nu_{LT} = 0.42$, $\nu_{TT} = 0.5$. The proposed CUF beam structural model makes use of four L9 polynomials (one for each wall of the box) to approximate the cross-section kinematics, whereas ten 4-node (cubic) beam finite elements are utilized along the longitudinal axis.

Figure 4a shows, in a graphical form, the natural frequencies related to some important vertical (VB) and horizontal (HB) bending mode shapes for various angles θ. Also, the figure compares the results by the present model, which is referred to as 4L9, with the analytical solution provided by Armanios and Badir [21]. Figure 4b shows the influence of θ on the natural frequencies related to twist-extension modes. According to the notation used in [21], S modes correspond to twist-extension modes which are dominated by the torsion (note that, when $\theta = 0$ deg, the mode S is purely torsional). On the contrary, the twist-extension modes which are dominated by extensional deformations are denoted to as P in Fig. 4b.

From the results given, it should be clear that ply angles up to 60 deg have a significant influence on the natural bending frequencies and the proposed beam model is in good agreement with the analytical reference solutions. Moreover, unlike S modes, the twist-extension modes dominated by extension (modes P) are significantly affected by θ in the case of the CUS box beam under consideration.

Reinforced composite wing box

A cantilever composite box is analyzed as the final example. It has rectangular cross-section as shown in Fig. 5. The length of the structure is 3.2 m. The material employed is a fibre reinforced orthotropic composite and has the following characteristics:

$E_1 = 141.96$ GPa, $E_2 = E_3 = 9.79$ GPa.
$\nu_{12} = \nu_{13} = 0.42$, $\nu_{23} = 0.5$.

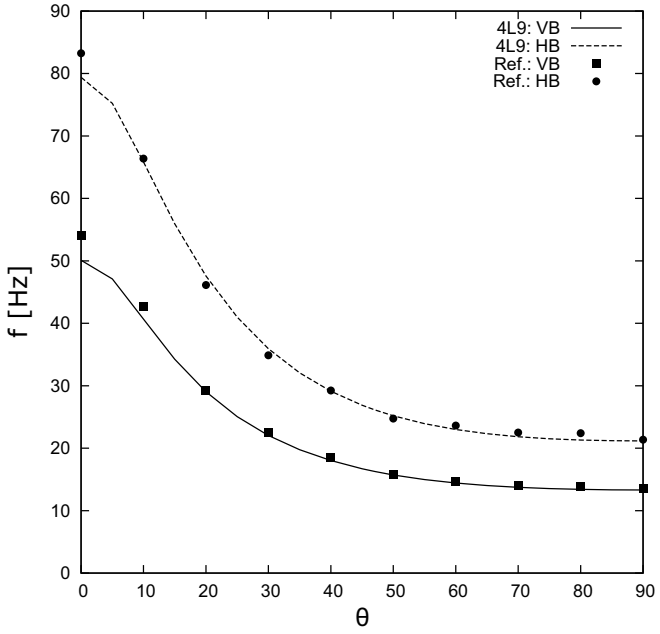

(a) Vertical (VB) and Horizontal (HB) bending modes by 4L9 and solution from [21]

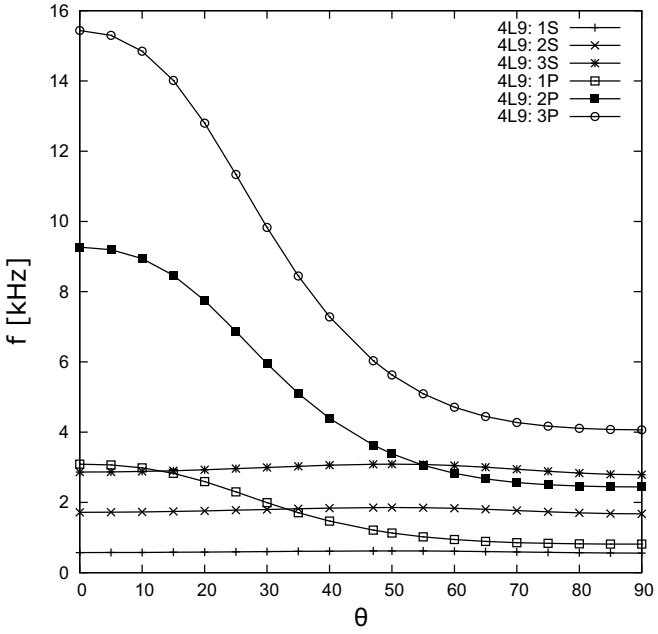

(b) Extension-twist coupled modes

FIGURE 4. NATURAL FREQUENCIES VS. PLY ANGLE FOR THE CUS BOX BEAMS WITH $[\theta]_6$ LAMINATION SCHEME.

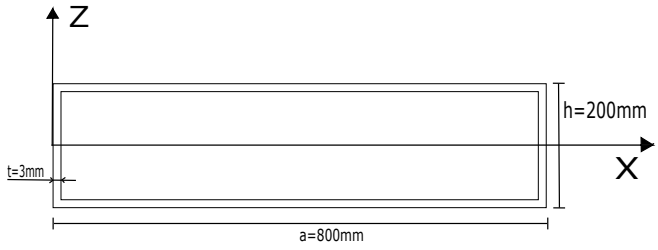

FIGURE 5. CROSS-SECTION OF THE COMPOSITE WING BOX.

$G_{12} = G_{13} = 6$ GPa, $G_{23} = 4.83$ GPa.
$\rho = 1445$ kg/m^3.

The box is simply compressed by a uniform load. In order to show the capabilities of the present approach to deal with complex geometries, two transverse reinforcements (ribs) are added. One rib is located at the free end of the beam, whereas the other one is at the mid-span. These ribs have thickness equal to 5 mm and they are made of an aluminium alloy ($E = 75$ GPa, $\nu = 0.33$, $\rho = 2700$ kg/m^3). The CUF-based CW model proposed in this section make use of 16 quadratic L9 polynomials to approximate the beam kinematics. Contrarily, 20 L9 polynomials are used for each rib. Along the beam axis 12 cubic (B4) beam elements are utilized.

First, the effect of the fiber orientation on buckling and free vibration analyses is investigated. Table 2 shows the different stacking sequences employed. The natural frequencies and the critical compressive loads for the various lamination configurations of the reinforced box are shown in Tables 3 and 4, respectively. The analysis highlights that:

- The natural frequencies decrease as the orientation angle increases (from 0° to 45°).
- Configurations B and C present similar results, both in terms of natural frequencies and critical buckling loads.
- Configuration F presents the highest values of critical loads

TABLE 2. STACKING SEQUENCES OF THE COMPOSITE WING BOX.

Orientation case	Wall			
	Top	Bottom	Left	Right
A	$[0]_2$	$[0]_2$	$[15]_2$	$[-15]_2$
B	$[15]_2$	$[-15]_2$	$[0]_2$	$[0]_2$
C	$[15]_2$	$[-15]_2$	$[15]_2$	$[-15]_2$
D	$[0]_2$	$[0]_2$	$[45]_2$	$[-45]_2$
E	$[45]_2$	$[-45]_2$	$[45]_2$	$[-45]_2$
F	$[0]_2$	$[0]_2$	$[90]_2$	$[-90]_2$
G	$[90]_2$	$[-90]_2$	$[0]_2$	$[0]_2$

TABLE 3. FIRST FIVE NATURAL FREQUENCIES [HZ] OF THE COMPOSITE BOX FOR VARIOUS LAMINATION SCHEMES; CW MODEL.

Mode	Lamination scheme						
	A	B	C	D	E	F	G
1	32.30	24.96	24.22	32.05	13.21	30.30	14.94
2	54.33	54.04	54.63	61.63	39.16	74.07	57.91
3	54.48	54.17	54.76	61.79	63.49	75.18	57.92
4	62.30	62.01	62.77	69.36	63.53	75.30	59.59
5	63.11	62.70	63.47	70.18	70.59	80.73	59.61

TABLE 4. FIRST FIVE CRITICAL BUCKLING LOADS [N] OF THE COMPOSITE BOX FOR VARIOUS LAMINATION SCHEMES; CW MODEL.

$P_{cr} \times 10^{-4}$	Lamination scheme						
	A	B	C	D	E	F	G
1	6.38	7.78	6.93	38.41	1.81	43.67	0.45
2	6.52	8.25	6.99	38.63	1.92	43.95	0.47
3	6.77	8.31	7.29	40.02	3.69	44.01	0.52
4	6.90	8.72	7.38	40.43	3.78	44.27	0.53
5	9.08	10.92	9.71	53.93	4.08	56.46	0.54

and natural frequencies. In this case, in fact, the load is applied in the direction of the fibres at the top and bottom walls. On the contrary, the same walls have fibres in the orthogonal direction with respect to the load in configuration G, which is therefore the most ineffective lamination configuration.

For the orientation configuration A, Fig. 6 shows the variation of the first eight natural frequencies versus the magnitude of the axial pre-stress P. It is easy to identify critical buckling loads as those loads that make the related natural frequency go to zero. The following comments arise from the analysis:

- Flexural modes (1 and 8) are not affected by axial pre-stresses, of course.
- There are various interesting dynamic phenomena: Crossing phenomena involve modes 2-3 with modes 4-5 as well as modes 6-7 with mode 8. During crossing, the modal deformations remain unaltered. On the other hand, mode shapes change sensibly after the veering zone at approximately $P = 40 \times 10^3$ N.

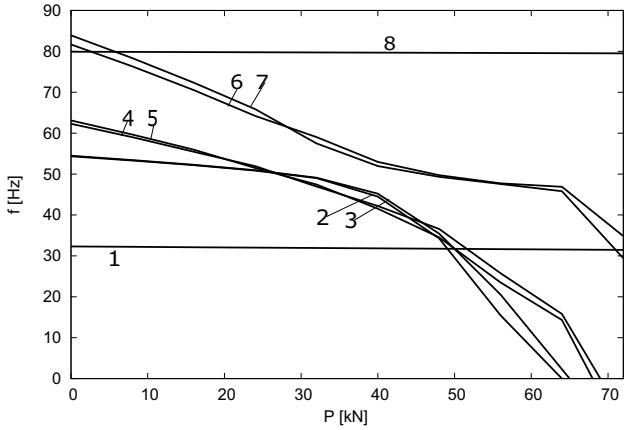

FIGURE 6. VARIATION OF THE NATURAL FREQUENCIES OF THE COMPOSITE WING BOX VS PRE-STRESS AXIAL LOAD; CW MODEL.

CONCLUSIONS

This paper has presented free vibration and linearized buckling analyses of reinforced composite structures for aerospace applications. The employed models are based on the 1D Carrera Unified Formulation (CUF). According to CUF, generalized higher-order beam models can be straightforward implemented by using a compact, index formulation that expresses the displacement field as the expansion of the primary unknowns by arbitrary cross-sectional functions. Namely, Lagrange polynomials have been utilized in this paper as cross-sectional functions and the finite element approach has been used for developing numerical applications. The use of Lagrange polynomial sets to define the kinematics of beam theories bring to the formulation of geometrically consistent models with Component-Wise (CW) capabilities. By considering simple plates to more complex composite reinforced box structures, the validity and the accuracy of the formulation proposed has been widely demonstrated.

REFERENCES

[1] Bruhn, E. F., 1973. *Analysis and Design of Flight Vehicle Structures*. Tri-State Offset Company.

[2] Rivello, R. M., 1969. *Theory and analysis of flight structures*. McGraw-Hill.

[3] Patel, S. N., Datta, P. K., and Seikh, A. H., 2006. "Buckling and dynamic instability analysis of stiffened shell panels". *Thin-Walled Structures,* ***44***, pp. 321–333.

[4] Vörös, G. M., 1988. "A special purpose element for shell-beam systems". *Computers and Structures,* ***29***(2), pp. 301–308.

[5] Vörös, G. M., 2007. "Finite element analysis of stiffened plates". *Periodica Polytechnica,* ***51***(2), pp. 105–112.

[6] Carrera, E., Giunta, G., and Petrolo, M., 2011. *Beam Struc-*

tures: Classical and Advanced Theories. John Wiley & Sons.

[7] Carrera, E., Cinefra, M., Petrolo, M., and Zappino, E., 2014. *Finite Element Analysis of Structures through Unified Formulation*. John Wiley & Sons, Chichester, West Sussex, UK.

[8] Carrera, E., Pagani, A., and Petrolo, M., 2013. "Classical, refined and component-wise theories for static analysis of reinforced-shell wing structures". *AIAA Journal,* ***51***(5), pp. 1255–1268.

[9] Carrera, E., Pagani, A., and Petrolo, M., 2013. "Component-wise method applied to vibration of wing structures". *Journal of Applied Mechanics,* ***80***(4), p. 041012.

[10] Carrera, E., Maiaru, M., and Petrolo, M., 2012. "Component-wise analysis of laminated anisotropic composites". *International Journal of Solids and Structures,* ***49***, pp. 1839–1851.

[11] Carrera, E., Filippi, M., Mahato, P. K. R., and Pagani, A., 2014. "Advanced models for free vibration analysis of laminated beams with compact and thin-walled open/closed sections". *Journal of Composite Materials,* ***49***(17), pp. 2085–2101.

[12] Carrera, E., Filippi, M., Mahato, P. K. R., and Pagani, A., 2016. "Accurate static response of single-and multi-cell laminated box beams". *Composite Structures,* ***136***, pp. 372–383.

[13] Carrera, E., and Pagani, A., 2014. "Free vibration analysis of civil engineering structures by component-wise models". *Journal of Sound and Vibration,* ***333***(19), pp. 4597–4620.

[14] Bathe, K. J., 1996. *Finite element procedure*. Prentice hall, Upper Saddle River, New Jersey, USA.

[15] Carrera, E., and Petrolo, M., 2012. "Refined beam elements with only displacement variables and plate/shell capabilities". *Meccanica,* ***47***(3), pp. 537–556.

[16] Carrera, E., Petrolo, M., Varello, A., Zappino, E., and Pagani, A., Forthcoming release. *Classical Aeroelasticity by Finite Element Method*. John Wiley & Sons.

[17] Zienkiewicz, O. C., and Taylor, R. L., 2005. *The Finite Element Method for Solid and Structural Mechanics*, 6th ed. Butterworth-Heinemann, Washington.

[18] Riks, E., 2004. "Buckling". *Encyclopedia of computational mechanics*.

[19] De Borst, R., Crisfield, M. A., Remmers, J. J. C., and Verhoosel, C. V., 2012. *Nonlinear finite element analysis of solids and structures*. John Wiley & Sons.

[20] Lekhnitskii, S., 1968. *Anisotropic Plates*. 2nd Edition, Translated from the 2nd Russian Edited by SW Tsai and Cheron, Bordon & Breach. Translated from 2nd Russian Edition.

[21] Armanios, E. A., and Badir, A. M., 1995. "Free vibration analysis of anysotropic thin-wall close-section beams". *AIAA Journal,* ***33***(10), pp. 1905–1910.